

A Simple Ultrasensitive Electrochemical Biosensor for Simultaneous Determination of Dopamine, Uric Acid and Ascorbic Acid Based on β -cyclodextrin/selenium Doped Carbon Quantum Dots Modified Glassy Carbon Electrode

Guojie Huang¹, Xiaoling Yang¹, Ruihui Huang, Zhihong Yan^{1,*}, Fuqiang Sun¹, Li Xu¹, Yi Liu^{1,2,*}

¹ College of Pharmacy, Guangdong Pharmaceutical University, Guangdong, China.

² School of Chemistry and Chemical Engineering, Guangdong Pharmaceutical University, Guangdong, China.

*E-mail: yzhxsp@aliyun.com, 1499088964@qq.com

Received: 10 May 2020 / Accepted: 17 July 2020 / Published: 31 August 2020

In this work, a novel electrochemical sensor for the simultaneous determination of ascorbic acid (AA), dopamine (DA) and uric acid (UA) was successfully prepared by using β -cyclodextrin (β -CD) / Se doped carbon quantum dots (Se-CQDs) modified glassy carbon electrode (GCE). The β -CD/Se-CQDs composite was characterized by the TEM and FTIR. The electrochemical behaviors of AA, DA and UA on the modified electrode were investigated by cyclic voltammetry, electrochemical impedance spectroscopy and differential pulse voltammetry. AA, DA, and UA can be separated well due to the synergistic effect of β -CD and Se-CQDs. The three oxidation peaks current were linearly with the concentration range of 10 ~ 1400 μ M, 60 ~ 1000 μ M and 10 ~ 1000 μ M for AA, DA, and UA, respectively, with the limits of detection of 0.06, 0.02, 0.03 μ M (S/N = 3). Moreover, as-prepared biosensor exhibited prominent selectivity, stability and reproducibility and it was used for the simultaneous determination of AA, DA, and UA in human serum and urine samples with satisfactory results.

Keywords: β -cyclodextrin, Carbon quantum dots, Ascorbic acid, Dopamine, Uric acid.

1. INTRODUCTION

Dopamine is the most abundant catecholamine neurotransmitter in the brain. Dopamine, as a neurotransmitter, regulates many physiological functions of the central nervous system [1-3]. The dysregulation of dopamine system involves Parkinson's disease, schizophrenia, Tourette's syndrome, attention deficit hyperactivity syndrome and pituitary tumor [4-6]. Therefore, real time monitoring of dopamine concentration is very important. AA, DA and UA coexist in biological systems and play an important role in physiological processes. Therefore, sensitive and selective detection methods for these

biomarkers are useful for studying their physiological functions and clinical diagnosis is required. [7]. The several methods was founded to determine DA, UA and AA and the electrochemical method was popular [8-12].

CQDs is a carbon-based zero-dimensional material, which has the advantages of excellent optical properties, good biocompatibility, a wide range of raw materials and low cost [13-16]. CQDs was widely used in many fields, medical imaging technology, environmental monitoring, chemical analysis, catalyst preparation, energy development, etc. [17-21]. CQDs can be used to structure electrochemical sensor [22-25].

β -CD is the product of starch cyclization. It can envelop a variety of compound molecules, increase the stability of the enveloped substance to photo-thermal and oxygen, and change the physical and chemical properties of the enveloped substance [26]. In the process of electrochemical reaction, the guest molecule can form inclusion complex with β -CD through electrostatic and van der Waals force, etc. [27, 28]. Hence, β -CD as a modified material can increase the sensitivity and selectivity of the sensor. [29-31].

We successfully fabricated a highly selective electrochemical sensor based on the β -CD and Se-CODs composite. The developed sensor can be used for determination of AA, DA and UA and it exhibited higher selectivity, wider liner range and excellent reproducibility.

2. MATERIALS AND METHODS

2.1. Reagents and chemicals

Citric acid (CA), sodium citrate, Na_2HPO_4 , NaH_2PO_4 , dopamine (DA), and uric acid (UA) were purchased from Shanghai Macklin Biochemical Co., Ltd., (Shanghai, China). L-ascorbic acid (AA) and sodium selenite were purchased from Nanjing Chemical Reagent Co., Ltd, (Nanjing, China). β -cyclodextrin (β -CD) was purchased from Chengdu Kelong Chemical Reagent Factory (Chengdu, China). Glycine and glucose were purchased from Nine-Dinn Chemistry (Shanghai) Co., Ltd., (Shanghai, China). NaCl and KCl were purchased from Guangzhou Chemical Reagent Factory (Guangzhou, China). Na_2SO_4 were purchased from Fuchen (Tianjin) Chemical Reagent Co., Ltd., (Tianjin, China). MgCl_2 was purchased from Damao Chemical Reagent Factory (Tianjin, China). $\text{K}_3\text{Fe}(\text{CN})_6$ was purchased from Shanghai Lingfeng Chemical Reagent Co., Ltd., (Shanghai, China). AA, DA and UA solutions were freshly prepared every day and stored at 4 °C when not in use. In addition, we use ultrapure water to produce all solutions. All reagents were of analytical grade.

2.2. Preparation of Se-CQDs

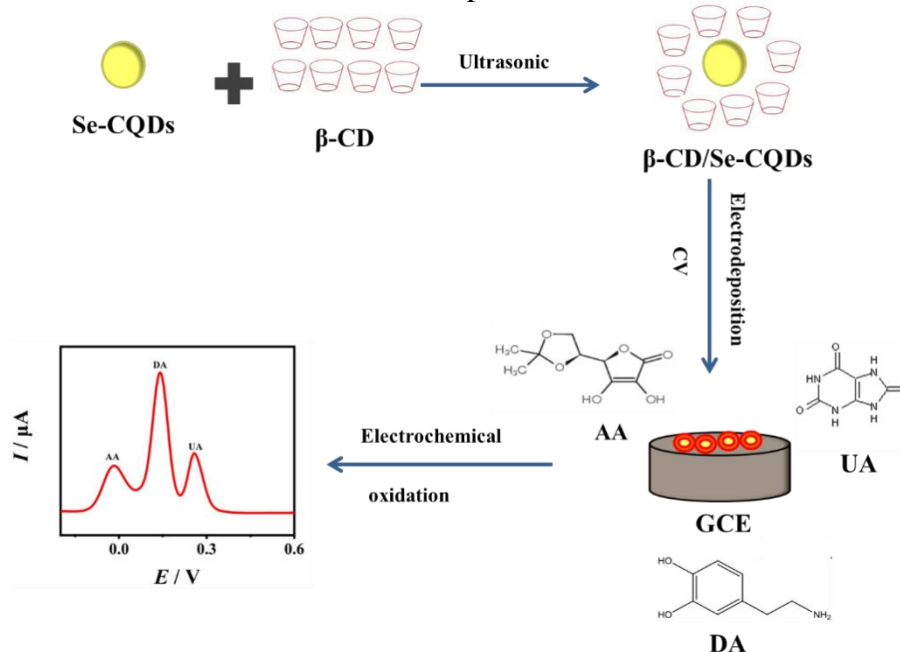
Weigh 5 g of citric acid and 0.06 g of sodium selenite dissolved in 40 mL of ultrapure water. After dissolving, transfer the solution to the PTFE lining, and then insert the PTFE lining into a stainless steel reactor, and react at 150°C for 150 min. After the reaction was completed, the reaction solution was

centrifuged at 8000 r/min for 20 min, and the supernatant was taken. Next, dialyze with a 200 Da dialysis bag for 2 days, change the water every 5 h, and finally freeze-dry to obtain Se-CQD.

2.3. Preparation of modified electrodes

Before modification, GCE was polished into mirror-like with 0.3 and 0.05 μm alumina powder, and then cleaned with ethanol and ultrapure water for 5 minutes each time.

0.04 g β -CD and 5 mL Se-CQDs (2 mg/mL) were added to 25 mL 0.1 M PBS (pH=6.5), and sonicated for 30 minutes to obtain a uniform β -CD/Se-CQDs mixed solution. In a β -CD/Se-CQDs mixed solution, 10 cycles were performed between -1.0 and 1.0 V by cyclic voltammetry (CV) with a scan rate of 50 mV s^{-1} , and β -CD/Se-CQDs/GCE. The prepared electrode was carefully washed thoroughly with double distilled water, and then dried under an infrared lamp. β -CD/GCE and Se-CQDs/GCE were obtained using similar methods. β -CD/GCE is obtained in β -CD solution by continuous CV 4 cycles between -1.0 ~ 1.0 V. The preparation of Se-CQDs/GCE is performed by continuous CV 20 cycles between 0 ~ 1.0 V in a Se-CQDs solution at a scan rate of 50 mV s^{-1} . The electrochemical behavior of the AA, DA and UA on the modified electrode was presented in the Scheme 1.



Scheme 1. The schematic routine for preparing β -CD/Se-CQDs/GCE.

2.4. Equipment and measurements

Transmission electron microscopy (TEM) was used to analyze the surface morphology of β -CD/Se-CQDs/GCE. Fourier-transform infrared spectroscopy (FTIR) measurement was performed using Perkin Elmer FTIR-Spectrum 400.

Cyclic voltammetry (CV), electrochemical impedance spectroscopy (EIS) and differential pulse voltammetry (DPV) measurements were obtained by the CHI660E electrochemical workstation, which was composed of a saturated calomel electrode reference electrode, a platinum sheet counter electrode,

and a bare or modified GCE as working electrode. The scanning potential of CV measurements was carried out between -0.2 V and 0.6 V with the scan rate at 100mV s^{-1} . And the sweep potential of DPV measurements was performed by from -0.2 V to 0.6 V. All of the measurements were recorded at room temperature.

3. RESULTS AND DISCUSSION

3.1. Characterization of Se-CQDs and as-prepared composite

The geometric structural features of the Se-CQDs (Fig. 1A) and β -CD/Se-CQDs (Fig. 1B) were characterized using TEM. The as-prepared Se-CQDs with an average diameter of 6.8 nm exhibit uniform sphere structure. It can be seen from Fig. 1B that Se-CQDs are wrapped with β -CD, indicating that β -CD/Se-CQDs can be successfully prepared by electrochemical polymerization.

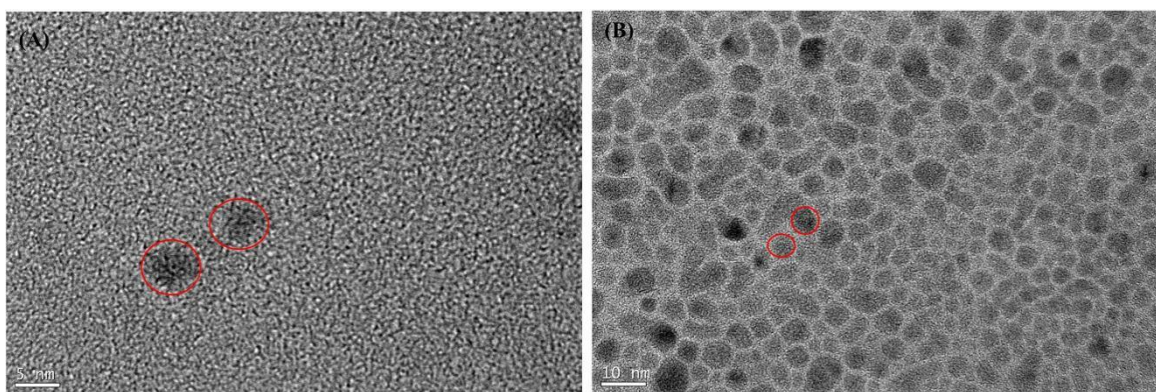


Figure 1. TEM images of Se-CQDs (A) and β -CD/Se-CQDs (B).

The β -CD/Se-CQDs were characterized by FTIR, and the results were shown in Fig. 2. The absorption peaks at $3000\sim 2900$ and $3600\sim 3100$ cm^{-1} are attributed to $-\text{CH}$ and $-\text{OH}$ stretching vibration of β -CD. The β -CD/Se-CQDs composites all have β -CD absorption peaks, indicating that β -CD can be combined with Se-CQDs. The results showed that β -CD/Se-CQDs were successfully prepared. [32].

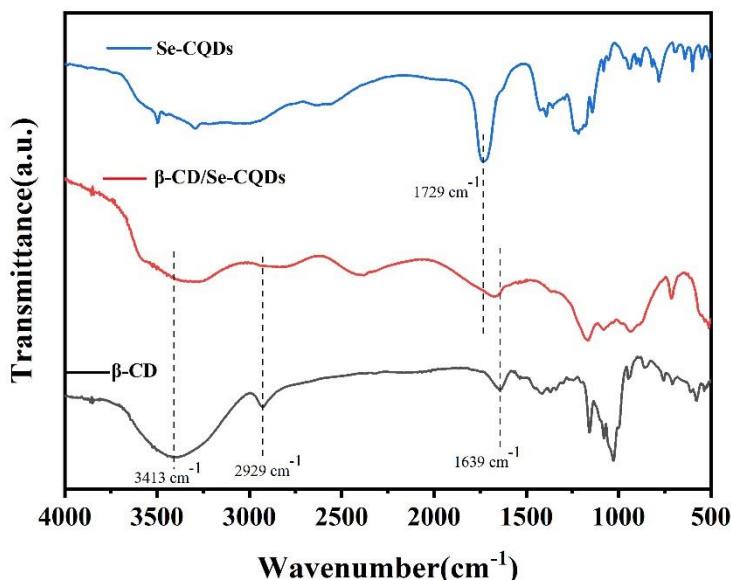


Figure 2. FT-IR pattern of β -CD, Se-CQDs, β -CD/Se-CQDs.

3.2. Electrochemical behaviors of AA, DA and UA

Shown in Fig. 3 were CVs (A) and DPVs (B) of AA, DA and UA in 0.1 M PBS (pH=6.5) and 42.5mM sodium citrate on bare/GCE, Se-CQDs/GCE and β -CD/Se-CQDs/GCE. Three oxidation peaks were obtained on the above three kinds of electrode. Comparatively, the oxidation peaks current were the most obvious on the β -CD/Se-CQDs/GCE and it is nearly 1.5 fold of the bare/GCE. The increased current was attributed to the synergistic effect of β -CD and CQDs. Moreover, the β -CD/Se-CQDs/GCE had prominent resolutions for the AA, DA and UA and the peak separations of AA-DA and DA-UA oxidation potentials were 152 and 116 mV, respectively.

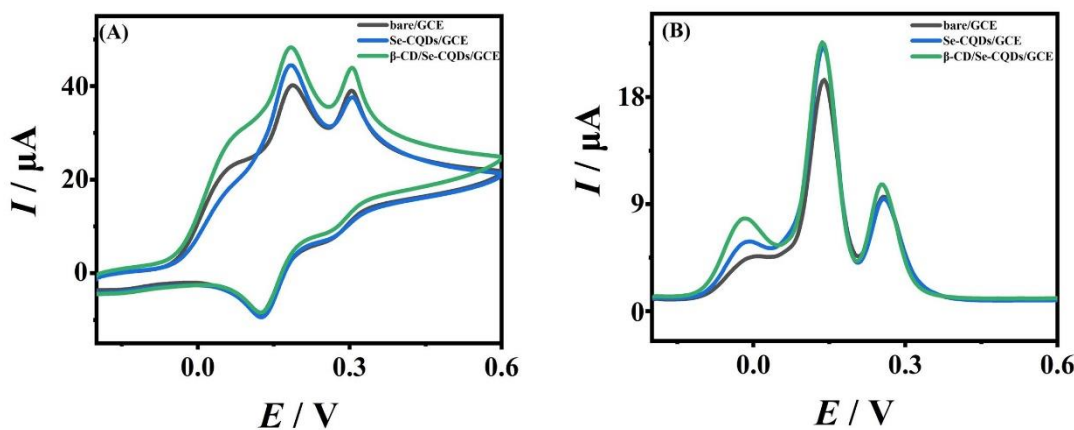


Figure 3. CVs(A) and DPVs(B) of 1mM AA, 0.5mM DA, 0.3mM UA on bare/GCE, Se-CQDs/GCE, β -CD/Se-CQDs/GCE in 0.1M PBS (pH=6.5) containing 42.5mM sodium citrate at a scan rate of 0.1V/s. Scan range from -0.2V to 0.6V.

3.3. Optimization of experimental conditions

3.3.1 Effect of pH on the determination of AA, DA and UA

Protons participated in the electrochemical reactions of AA, DA and UA on the modified electrode owe to there are multiple hydroxyl and amino. And then the effect of pH of supporting electrolyte was investigated is necessary. As shown in Fig. 4C, the oxidation peaks potential (E_{pa}) linearly shifted negatively with the pH range of 6.2-8.0. The relevant linear regression equations were $E_{pa, DA}/(V) = 0.4743 - 0.0516pH$, $E_{pa, UA}/(V) = 0.5841 - 0.05pH$, with correlation coefficients of 0.9964, 0.9931, respectively. The slops of the above regression equations near to the $59\text{ mV } pH^{-1}$ indicated that two proton and two electron transfer process during the electrochemical reactions of DA and UA [33]. As for AA (Fig. 5C), The relevant linear regression equations were $E_{pa, AA}/(V) = 0.6096 - 0.0897pH$, with correlation coefficients of 0.9818. A slop of $89.7\text{ mV } pH^{-1}$ is close to that given by the Nest equation for non-equal number for two electrons and one proton transfer process [34]. Moreover, the oxidation peaks current (I_{pa}) was affected by the pH of the buffer solution. The pH 6.5 was the most choice in the experiment according to the higher peak current and the better resolution and the results were shown in the Fig. 4B and Fig. 5B.

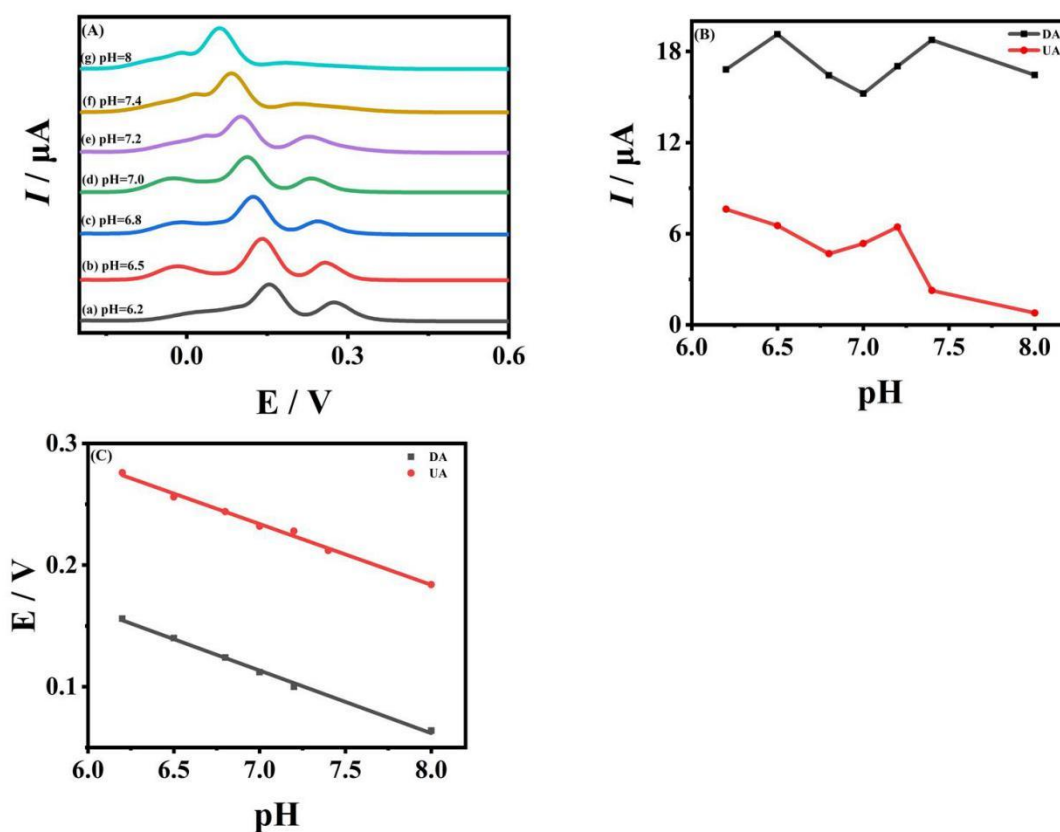


Figure 4. (A) DPV was used to measure the current response of 0.5mM DA and 0.3mM UA at different pH values; the effect of pH on the peak current (B) and peak potential (C) of 0.5mM DA and 0.3mM UA on β -CD/Se-CQDs/GCE.

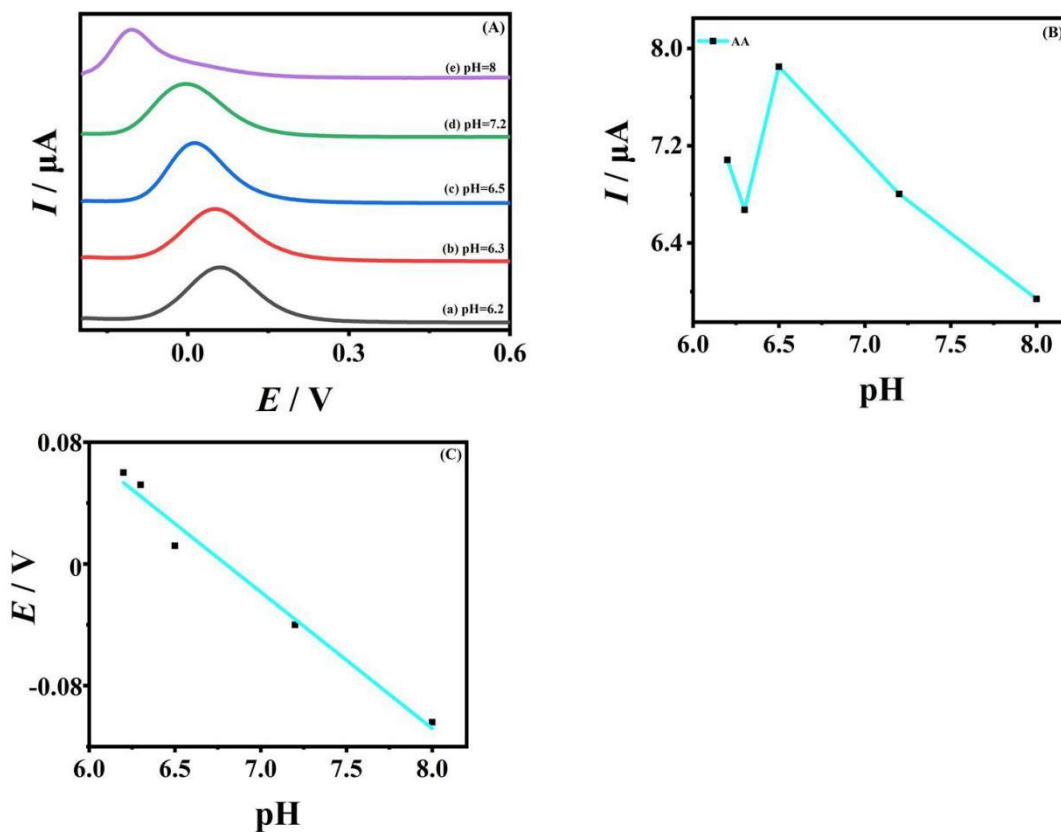


Figure 5. (A) DPVs of AA (1mM) at β -CD/Se-CQDs/GCE from 0.1M PBS with different pH values range of 6.2–8.0; (B) Plots of the oxidation peak currents for AA as function of solution pH; (C) Effects of solution pH values on peak potentials of AA at β -CD/Se-CQDs/GCE.

3.3.2 Effect of scan rate on the simultaneous determination

The change of scan rate can directly affect the electrochemical reactions [35]. Hence the effect of scan rate on the catalytic oxidation of AA, DA and UA on the β -CD/Se-CQDs/GCE was studied. The results were shown in the following figures. As shown in Fig. 6A were CVs of AA, DA and UA in the 0.1 M PBS (pH6.5) with the different scan rates between 20-500 mV s^{-1} . The I_{pa} was linearly increasing with the scan rates enlarged and the corresponding regression equation are: for DA (Fig. 6B), $I_{\text{pa, DA}}/(\mu\text{A}) = 0.1896 + 0.1472 v/(\text{mVs}^{-1})$; for AA (Fig. 6C), $I_{\text{pa, AA}}/(\mu\text{A}) = 6.3478 - 0.0091 v/(\text{mVs}^{-1})$ and for UA (Fig. 6D), $I_{\text{pa, UA}}/(\mu\text{A}) = 3.5314 + 0.0419 v/(\text{mVs}^{-1})$ with correlation coefficients of 0.9902, 0.9653 and 0.9955, respectively, which proved that the electrochemical reactions were controlled by the adsorption [36]. Furthermore, the E_{pa} of AA, DA and UA were shifted positively with the increasing of scan rates (Fig. 6E). The E_{pa} was linearly with the logarithm of scan rates and the regression equations are $E_{\text{pa, DA}}/(\mu\text{A}) = 0.1152 + 0.393 \log v/(\text{mVs}^{-1})$, $E_{\text{pa, AA}}/(\mu\text{A}) = -0.0086 + 0.03380 \log v/(\text{mVs}^{-1})$ and $E_{\text{pa, UA}}/(\mu\text{A}) = 0.2423 + 0.0344 \log v/(\text{mVs}^{-1})$ with correlation coefficients of 0.9902, 0.9894 and 0.9909, respectively. Therefore, the electrochemical reactions of AA, DA and UA on the β -CD/Se-CQDs/GCE were ascribed to adsorption-controlled and irreversible electrode process.

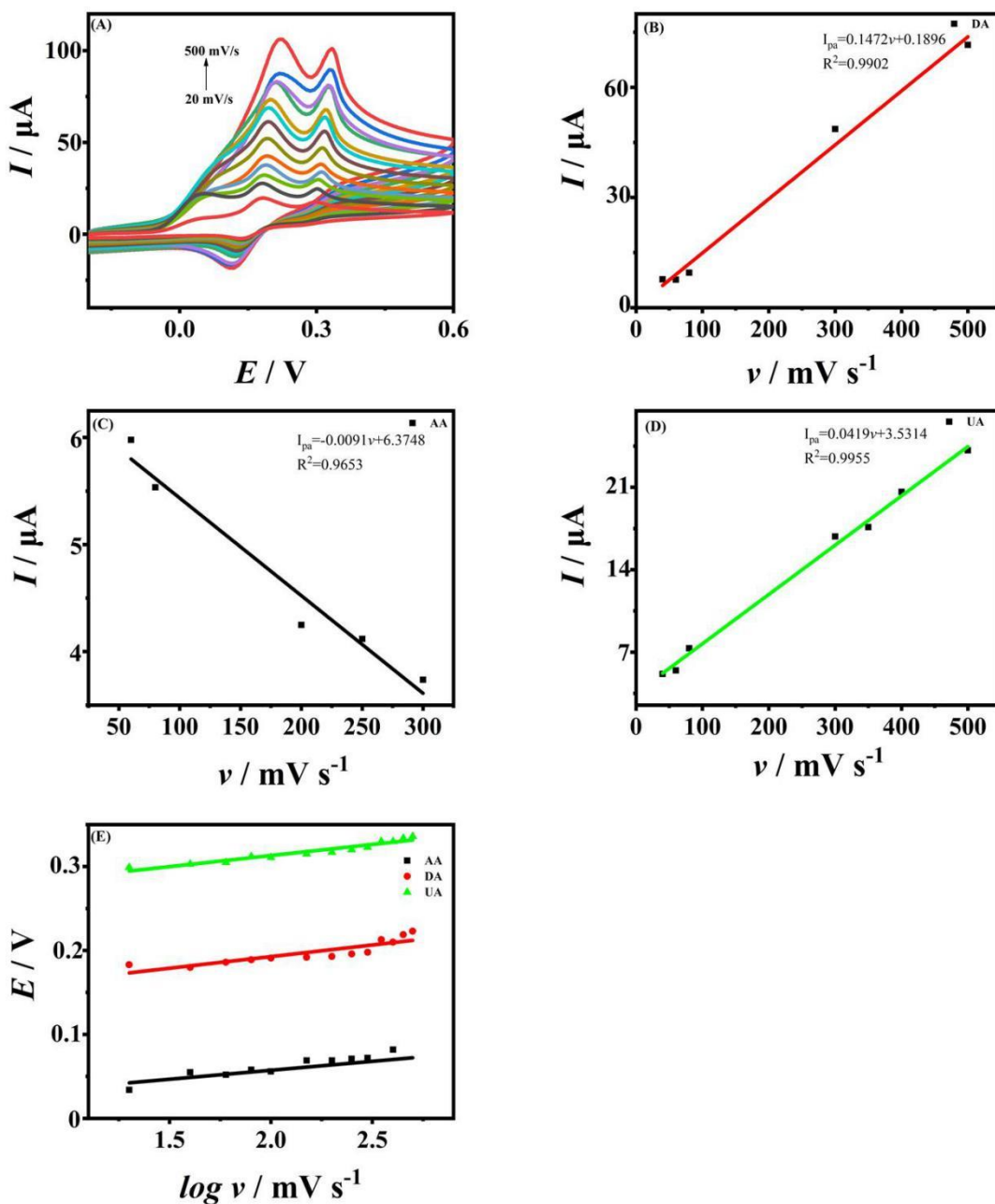


Figure 6. CVs(A) of the β -CD/Se-CQDs/GCE in 0.5mM DA, 0.3mM UA, 1mM AA at different scan rates of 20, 40, 60, 80, 100, 150,200,250,300,350,400,450 and 500 mV s^{-1} . Plots of anodic peak currents recorded at β -CD/Se-CQDs/GCE of (B) DA, (C) AA, (D) UA. (E) Plots of peak current versus the logarithm of scan rate.

3.4. Simultaneous determination of AA, DA and UA

3.4.1. Selectivity of AA, DA, and UA detection by β -CD/Se-CQDs/GCE

The calibration curves of AA, DA and UA were studied by DPVs as shown in Fig. 7. Briefly speaking, concentration of one substance changed, while the other two species remained constant during the process of testing.

As shown in Fig. 7A-B, I_{pa} of DA increased linearly with the increasing of DA concentration and the concentration of the other two substances was not changed. And then the linear range was found between 60 to 1000 μ M with the detection limit of 0.02 μ M. The linear equation of $I_{pa, DA}/(\mu A) = 0.044 + 26.203c/(mM)$ with correlation coefficient of 0.9954 was obtained. I_{pa} of AA increased linearly with the increasing of AA concentration range from 10 to 1400 μ M (Fig. 7C-D).

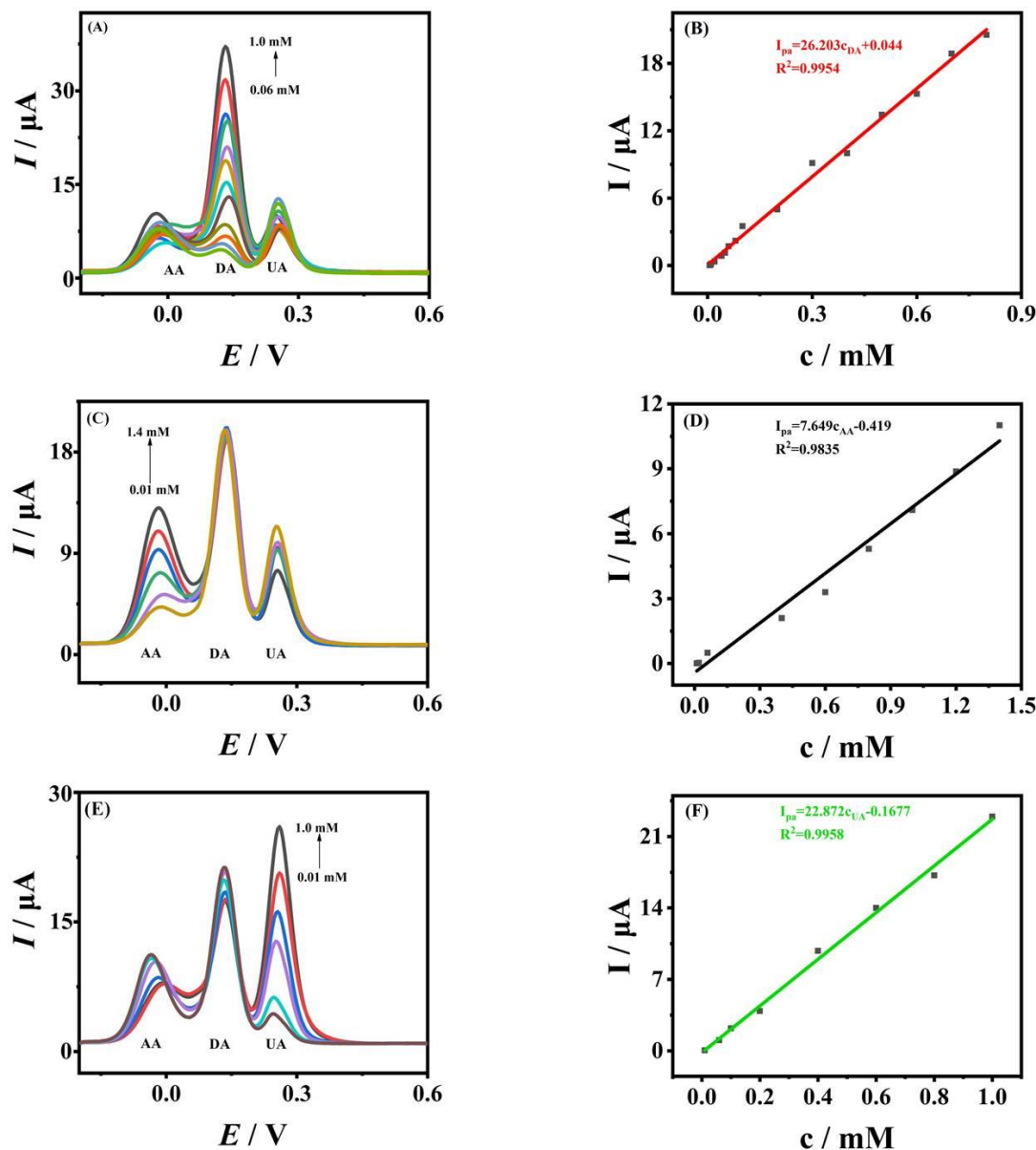


Figure 7. (A, C, E) DPV curves of DA, AA and UA of different concentrations at β -CD/Se-CQDs/GCE in 0.1 MPBS (pH 6.5). From bottom to up the concentrations of DA: 60–1000 μ M, AA: 10–1400 μ M and UA: 10–1000 μ M. (B, D, F) Oxidation peak current graphs corresponding to DA, AA, and UA concentrations, respectively.

The linear regression equation was expressed as $I_{pa, AA}/(\mu A) = -0.419 + 7.649c/(mM)$ with correlation coefficient of 0.9835 and the detection limit of AA is 0.06 μ M. Fig. 7E-F showed the DPVs of UA with different concentration keeping the concentration of AA and DA constant. The results

showed that the peak current of UA was linearly with the concentration of UA from 10 to 1000 μ M with the detection limit of 0.03 μ M. The related regression equation was expressed as $I_{pa, UA} (\mu A) = 0.1677 + 22.872c / (mM)$ with correlation coefficient of 0.9958.

3.4.2. Interference, reproducibility and stability study of sensor

There is a variety of interference coexisting in biological samples. As shown in Fig. 8, the interference of some possible substances on the simultaneous determination of AA, DA and UA by β -CD/Se-CQDs/GCE was studied. When the concentration of glycine, glucose, Mg^{2+} , SO_4^{2-} , Na^+ and Cl^- was more than 25 times, the peak current was not affected.

To examine the reproducibility of the proposed the sensor, the responses to the mixture of AA (1mM), DA (0.5mM) and UA (0.3mM) was measured by DPV. The related standard deviations (RSD) for AA, DA and UA are 1.59%, 0.2%, 5.57% after 6 times successive test. The results showed that the developed method has good reproducibility.

The stability is a key indicator to measure the performance of sensor. Therefore, the developed sensor was stored to the refrigerator for 7 days and the β -CD/Se-CQDs/GCE was used to determine AA (1mM), DA (0.5mM) and UA (0.3mM) mixture solution. The I_{pa} of AA, DA and UA can remain 92.5%, 92.3%, 95.7% of origin response, respectively, which indicates that the sensor has good stability.

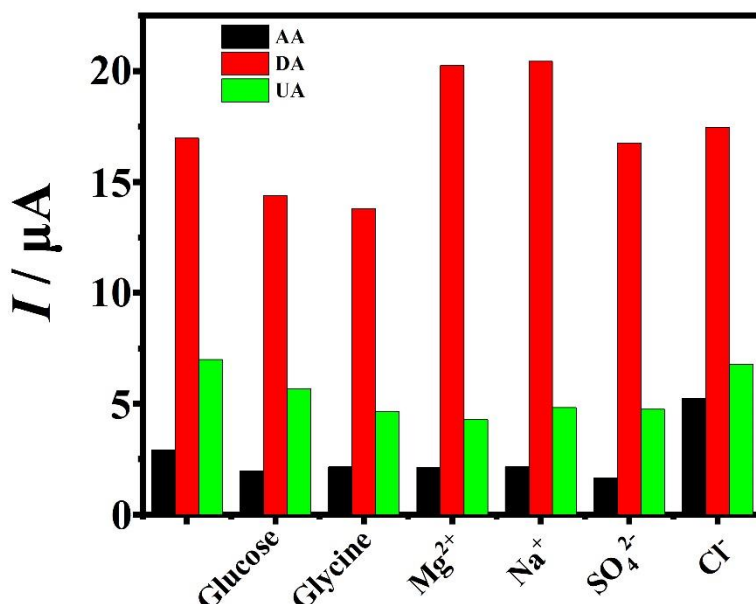


Figure 8. The influence for AA (1mM), DA (0.5mM) and UA (0.3mM) from following compounds (25m M): glycine, glucose, Mg^{2+} , Na^+ , SO_4^{2-} , Cl^- .

In addition, Table 1 shows the analysis performance of β -CD/Se-CQDs/GCE compared with other work. It was obvious that as-prepared β -CD/Se-CQDs/GCE exhibited satisfactory performance.

Table 1. Performances of different biosensors for simultaneous detection of DA, UA and AA.

Electrode	Linear range (μM)			LOD (μM)			Ref.
	AA	DA	UA	AA	DA	UA	
rGO / ZnO ^a	50–2350	3–330	1–70	3.71	1.08	0.33	[36]
PIlox-GO ^b	75–2275	12–278	3.6–250	18.00	0.63	0.59	[37]
CNTs/CFE ^c	25.6-2000.3	5.0-120.6	20.0-800	10.00	0.03	0.60	[38]
ZnNi NPs@f-MWCNT ^d	300-1100	200-1200	200-1100	0.511	0.0655	0.0882	[39]
PPy hydrogel/GCE ^e	2.5–1500	0.08–250	0.25–400	1.283	0.0440	0.0460	[40]
3DGH-Fc/GCE ^f	20-450	10-180	8-400	0.18	0.04	0.07	[41]
Pd Au/RGO/GCE ^g	12.5-700	1.25-73.75	2.5-66.25	12.50	0.75	2.50	[42]
BN/GCE ^h	30-1000	0.5-150	1-300	3.77	0.02	0.15	[43]
3DGH-AuNPs/GCE ⁱ	1.0-700	0.2-30	1-60	0.028	0.0026	0.005	[44]
ERGO/GCE ^j	300–2000	0.5–60	0.5–60	300	0.50	0.50	[45]
β -CD/Se-CQDs	10-1400	60-1000	10-1000	0.06	0.02	0.03	This work.

^a rGO/ZnO: reduced graphene oxide-zinc oxide.

^b PIlox-GO: overoxidized polyimidazole and graphene oxide copolymer.

^c CNTs/CFE: carbon nanotube/carbon fiber electrodes.

^d ZnNi NPs@f-MWCNT: ZnNi bimetallic nanoalloy @ functional multiwalled carbon nanotube.

^e PPy hydrogel: 3D networked polypyrrole hydrogel.

^f 3DGH-Fc: ferrocene hybrid/three dimensional graphene hydrogel nanocomposite.

^g PdAu/RGO: PdAu/grapheme nanocomposites.

^h BN: Flake hexagonal boron nitride.

ⁱ 3DGH-AuNPs: three-dimensional graphene hydrogel and gold nanoparticles nanocomposite.

^j ERGO: electrochemically reduced graphene oxide.

3.5. Real serum and urine samples analysis

In order to evaluate the value of the practical application of the proposed method, serum and urine samples were used for analysis by the developed method using the standard addition technique. The serum and urine samples were diluted 100 and 20 times with 0.1 M PBS (pH=6.5) solution, respectively. After adding a certain amount of AA, DA and UA, the sample dilution was transferred to an electrochemical cell and analyzed by DPV. The results are summarized in Table 2. It should be noted that the recovery of serum samples is 90~111.8%, and the relative standard deviation is 0.5~9.1%; the recovery of urine samples is 92.9~110.8%, and the relative standard deviation is 0.9~7.4%. The results of detection proved that the proposed sensor has great value of practical application.

Table 2. Detection results of AA, DA and UA in real samples (n=3).

	Detected (μM)	Added (μM)	Found (μM)	Recovery (%)	RSD (%)
Serum					
DA	-	6	6.0	100.5	9.1
		12	11.8	98.3	8.1
		18	16.2	90	2.5
UA	10.3	5	15.9	103.9	2.3
		10	19.9	98.1	3.5
		15	23.1	91.3	1.5
AA	-	50	55.9	111.8	0.5
		100	93.6	93.6	5.8
		150	147.6	98.4	7
Urine					
DA	-	50	53.5	107.1	7
		100	110.8	110.8	4.1
		150	153.7	102.5	2.2
UA	289.4	140	404.6	94.2	3.7
		280	571.5	100.4	7.4
		420	658.9	92.9	0.9
AA	55.6	100	149.8	96.3	7.2
		200	255.4	99.9	3.8
		300	369.6	104	4.8

4. CONCLUSIONS

In summary, the β -CD/Se-CQDs composite modified electrode was successfully prepared by electrochemical polymerization, which can be used for the simultaneous analysis of AA, DA and UA in actual serum and urine samples with satisfactory results. The developed sensor possessed higher selectivity, excellent reproducibility and good stability. Therefore, comparison of other sensor performances modified by the different materials, the proposed sensor exhibited wider linear range and lower detection limit.

ACKNOWLEDGMENTS

This work was supported by the Guangdong Provincial Project (2016A010103039), Guangzhou Yuexiu District Science and Technology Plan Project (2017-WS-016), Guangdong Provincial Innovation and Entrepreneurship Training Program for College Students (S201910573034).

References

1. R.A. Mitchell, N. Herrmann, K.L. Lanctot, *CNS Neurosci. Ther.*, 17 (2011) 411.
2. P.J. Gaskill, D.R. Miller, J. Gamble-George, H. Yano, H. Khoshbouei, *Neurobiol. Dis.*, 105 (2017) 51.

3. M. Ahn, J. Kim, *J. Electroanal. Chem.*, 683 (2012) 75.
4. A. Abbaspour, A. Noori, *Biosens. Bioelectron.*, 26 (2011) 4674.
5. J.A. Ribeiro, P.M.V. Fernandes, C.M. Pereira, F. Silva, *Talanta*, 160 (2016) 653.
6. E. Farjami, R. Campos, J.S. Nielsen, K.V. Gothelf, J. Kjemis, E.E. Ferapontova, *Anal. Chem.*, 85 (2012) 121.
7. R. Aguilar, M.M. Davila, M.P. Elizalde, J. Mattusch, R. Wennrich, *Electrochim. Acta*, 49 (2004) 851.
8. Y.F. Zhao, Y.Q. Gao, D.P. Zhan, H. Liu, Q. Zhao, Y. Kou, Y.H. Shao, M.X. Li, Q.K. Zhuang, Z.W. Zhu, *Talanta*, 66 (2005) 5.
9. J. Wu, J. Suls, W. Sansen, *Electrochem. Commun.*, 2(2000) 90.
10. X. Yang, J. Kirsch, A. Simonian, *J. Microbiol. Methods*, 95 (2013) 48.
11. X. Yang, J. Kirsch, E.V. Olsen, J.W. Fergus, A.L. Simonian, *Sens. Actuators, B.*, 177 (2013) 659.
12. Z.H. Wang, J.F. Xia, L.Y. Zhu, F.F. Zhang, X.M. Guo, Y.H. Li, Y.Z. Xia, *Sens. Actuators, B.*, 161 (2012) 131.
13. P. Gong, L. Sun, F. Wang, X. Liu, Z. Yan, M. Wang, L. Zhang, Z. Tian, Z. Liu, J. You, *Chem. Eng. J.*, 356 (2019) 994.
14. W.S. Zou, Y.J. Ji, X.F. Wang, Q.C. Zhao, J. Zhang, Q. Shao, J. Liu, F. Wang, Y.Q. Wang, *Chem. Eng. J.*, 294 (2016) 323.
15. M. Zhang, W. Wang, P. Yuan, C. Chia, J. Zhang, N. Zhou, *Chem. Eng. J.*, 330 (2017) 1137.
16. H.Z. Xie, J. Dong, J.L. Duan, G.I.N. Waterhouse, J.Y. Hou, S.Y. Ai, *Sens. Actuators, B.*, 259(2018) 1082.
17. J. Dong, K. Wang, L. Sun, B. Sun, M. Yang, H. Chen, Y. Wang, J. Sun, L. Dong, *Sens. Actuators, B.*, 256 (2018) 616.
18. D. Tang, J. Liu, X. Wu, R. Liu, X. Han, Y. Han, H. Huang, Y. Liu, Z. Kang, *ACS Appl. Mater. Interfaces*, 6(2014) 7918.
19. Z.L. Peng, X. Han, S.H. Li, A. O.Al-Youbi, A.S. Bashammakh, M.S. El-Shahawi, R.M. Leblanc, *Coord. Chem. Rev.*, 343(2017) 256.
20. T. Liu, J.X. Dong, S.G. Liu, N. Li, S.M. Lin, Y.Z. Fan, J.L. Lei, H.Q. Luo, N.B. Li, *J. Hazard. Mater.*, 322(2017) 430-436.
21. X. Li, M. Rui, J. Song, Z. Shen, H. Zeng, *Adv. Funct. Mater.*, 25(2015) 4929.
22. N. Hashemzadeh, M. Hasanzadeh, N. Shadjou, J. Eivazi-Ziaei, M. Khoubnasabjafari, A. Jouyban, *J. Pharm. Anal.*, 6(2016) 235.
23. K. Yin, A. Liu, S.G. Li, M. Li, X. Liu, Y.J. Liu, Y.W. Zhao, Y. Li, W. Wei, Y.J. Zhang, S.Q. Liu, *Biosens. Bioelectron.*, 90 (2017) 321.
24. X. Zhuang, H. Wang, T. He, L. Chen, *Microchim. Acta*, 183(2016) 3177.
25. Y. Jiang, B. Wang, F. Meng, Y. Cheng, C. Zhu, *J. Colloid Interface Sci.*, 452(2015) 199.
26. M. Pérez Abril, C. Lucas Abellán, J. Castillo Sánchez, H. Pérez Sánchez, J.P. Cerón Carrasco, I. Fortea, J.A. Gabaldón, E. Núñez-Delicado, *J. Funct. Foods*, 36 (2017) 122.
27. E.M. Martin Del Valle, *Process Biochem.*, 39 (2004) 1033
28. .P. Mura, *J. Pharm. Biomed. Anal.*, 101(2014) 238.
29. H.Y. Zhao, X.P. Ji, B.B. Wang, N. Wang, X.R. Li, R.X. Ni, J.J. Ren, *Biosens. Bioelectron.*, 65(2015) 23.
30. S. Palanisamy, B. Thirumalraj, S.M. Chen, *J. Electroanal. Chem.*, 760(2016) 97.
31. M. Zhang, H.T. Zhao, X. Yang, A.J. Dong, H. Zhang, J. Wang, G.Y. Liu, X.C. Zhai, *Sens. Actuators, B.*, 229(2016) 190.
32. J.C. Chan, P. He, H.M. Bai, S.Y. He, T.H. Zhang, X.Q. Zhang, F.Q. Dong, *Sens. Actuators, B.*, 252(2017) 9.
33. Y. Yue, G. Hu, M. Zheng, Y. Guo, J. Cao, S. Shao, *Carbon*, 50(2012) 107.
34. D. Zhang, L. Li, W. Ma, X. Chen, Y. Zhang, *Mater. Sci. Eng., C*, 70(2016) 241.
35. Y-T. Shieh, H-F. Jiang, *J. Electroanal. Chem.*, 736(2015) 132.

36. X. Zhang, Y.C. Zhang, L.X. Ma, *Sens. Actuators, B.*, 227(2015) 488.
37. X.F. Liu, L. Zhang, S. Wei, S.H. Chen, *Biosens. Bioelectron.*, 57(2014) 232.
38. Y.F. Zhao, Z. Yang, W.X. Fan, Y.C. Wang, G.Z. Li, H.L. Cong, H. Yuan, *Arabian J. Chem.*, 13(2020) 3266.
39. A. Savk, B. Özdil, B. Demirkan, *Mater. Sci. Eng., C*, 99(2019) 248.
40. M.L. Wang, M.Z. Cui, W.F. Liu, X.G. Liu, *J. Electroanal. Chem.*, 832(2019) 174.
41. Q. Zhu, J. Bao, D.Q. Huo, M. Yang, H.X. Wu, *J. Electroanal. Chem.*, 99 (2017) 459.
42. C. Zou, J.T. Zhong, S.M. Li, H.W. Wang, *J. Electroanal. Chem.*, 805(2017) 110.
43. Q. Li, C.R. Huo, L.L. Zhou, L. Su, *Sens. Actuators, B.*, 260(2018) 346.
44. Q. Zhu, J. Bao, D.Q. Huo, M. Yang, C.J. Hou, J.F. Guo, *Sens. Actuators, B.*, 238(2017) 1316.
45. L. Yang, D. Liu, J. Huang, *Sens. Actuators, B.*, 193(2014) 166.

© 2020 The Authors. Published by ESG (www.electrochemsci.org). This article is an open access article distributed under the terms and conditions of the Creative Commons Attribution license (<http://creativecommons.org/licenses/by/4.0/>).